

Proceedings of Meetings on Acoustics

Volume 18, 2012

<http://acousticalsociety.org/>

164th Meeting of the Acoustical Society of America

Kansas City, Missouri

22 - 26 October 2012

Session 1aPA: Physical Acoustics

1aPA11. Partial field decomposition of jet noise sources using optimally located virtual reference microphones

Alan T. Wall*, Kent L. Gee, Tracianne B. Neilsen and Michael M. James

***Corresponding author's address: Department of Physics and Astronomy, Brigham Young University, N283 ESC, Provo, Utah 84663, alantwall@gmail.com**

It is desirable to isolate independent noise sources in jets for targeted noise reduction methodologies. The application of traditional partial field decomposition (PFD) techniques to jet noise fields is useful for estimating the number of incoherent (equivalent) noise sources within a jet and for implementing near-field acoustical holography, but it does not generally provide physically meaningful partial fields (i.e. partial fields related to individual sources). The method developed by Kim et al. [JASA 115(4), 2004] finds the optimal locations of references in a sound field and places virtual references at those locations. In past investigations this method has been successfully applied to locate discrete numerical and physical sources and to generate partial fields related to each source. In this study, Kim's method is applied to a full-scale jet installed on a military aircraft to obtain physically meaningful partial fields. [Work supported by ONR.]

Published by the Acoustical Society of America through the American Institute of Physics

1. Introduction¹

This work was presented at the 164th Meeting of the Acoustical Society of America in Kansas City, Missouri, 22-26 October 2012, under the title “Partial field decomposition of jet noise using optimally located virtual reference microphones.”

Jet noise emitted by military aircraft is a major source of hearing loss for military personnel, especially those who work on the deck of an aircraft carrier. The overall jet-noise source region is comprised of an ambiguous number of extended, partially spatially coherent subsources. It is desirable to isolate and identify the individual contributions of independent source components to the overall field, so that the development of noise-reduction methods may be targeted towards specific, physical source mechanisms. This work is an attempt to isolate the individual components of jet noise as a step toward the identification of independent source mechanisms.

More than six decades of research have gone into understanding the acoustic source mechanisms of turbulent mixing noise in jets. One analysis tool that has been employed is the partial field decomposition (PFD) of sound fields, based on the theory of principal component analysis,^{1,2} in conjunction with near-field acoustical holography (NAH).³⁻⁷ Through the use of a linear projection of the sound field onto a linearly independent basis set, PFD allows for the decomposition of a total sound field onto a set of mutually incoherent partial fields, the sum of which returns the magnitude of total sound field. In a scan-based measurement, where the entire aperture of “field” signals is comprised of a series of small, dense measurements, the scans are performed simultaneously with measurements at a fixed-location “reference” array. The signals measured at these reference microphones serve as the basis for the PFD.

Various PFD methods have been applied to jet noise fields,^{3,4,6,8,9} but the resulting partial fields are generally not “physically meaningful.” This is because members of the basis set onto which the sound field is projected do not typically represent signals from independent source components. In general, each transducer receives signals from multiple subsources. The PFD applications which most successfully generate physically relevant partial fields are performed with a set of reference transducers that are located close to individual subsources, which emphasizes the contribution of a single source to each reference signal. However, in consideration of a jet noise source, the distribution of partially coherent source regions precludes such a reference deployment.

Kim *et al.*¹⁰ developed a method that is called here the optimized-location virtual reference method (OLVR), which is a post-NAH PFD procedure that makes it possible to identify optimal reference sensor locations and then to place “virtual references” at those locations. Other methods that utilize virtual references exist,¹¹⁻¹³ but this one was developed specifically to find the optimal virtual reference locations. The optimal locations are defined as those at which the multiple signal classification (MUSIC) power¹⁴ is maximized in the three-dimensional region near the source. The necessary sound pressures for the MUSIC algorithm are obtained from a projection of the measured sound field toward the source with NAH. The projected pressure signals at these optimal locations then serve as the “virtual” reference signals. When the sound field is decomposed using the virtual reference signals as a basis set, the result is a set of physically meaningful partial fields.

Holographic projection of the jet noise field for a full-scale military aircraft was done previously.³ In this study, a PFD of these data are performed using OLVR. Section 2 provides a brief overview of the OLVR implementation procedure that is employed in this work. It is based mostly on the theoretical development offered by Kim *et al.*¹⁰ with minor modifications to accommodate a partially coherent, distributed source. Much of the

¹ SBIR DATA RIGHTS. Distribution A – Approved for Public Release; Distribution is Unlimited 88ABW-2012-5058. (See Acknowledgments for full statement.)

underlying theory is therefore passed over in this summary, in favor of a methodological outline. The full-scale jet noise experiment on which the OLVR analysis was performed is summarized in Section 3. Detailed descriptions of the experiment are provided in References 15 and 16. In Section 4, OLVR is applied to a full-scale jet. The NAH reconstructions, virtual reference selections, and decomposition of the field into physically meaningful partial fields are shown. Conclusions are provided in Section 5.

2. Methodology

The OLVR procedure relies on the sub-processes of back propagation toward the source through the use of NAH, a singular-value-decomposition (SVD) based PFD method,^{12,13} the MUSIC algorithm,¹⁴ and the Gauss elimination technique (Cholesky decomposition) that is integral to the partial coherence decomposition PFD method (PCD).¹⁷ In the following discussion of each step, it may be helpful for the reader to refer to the process outlined in Fig. 1. Note that the OLVR process is performed independently for each frequency.

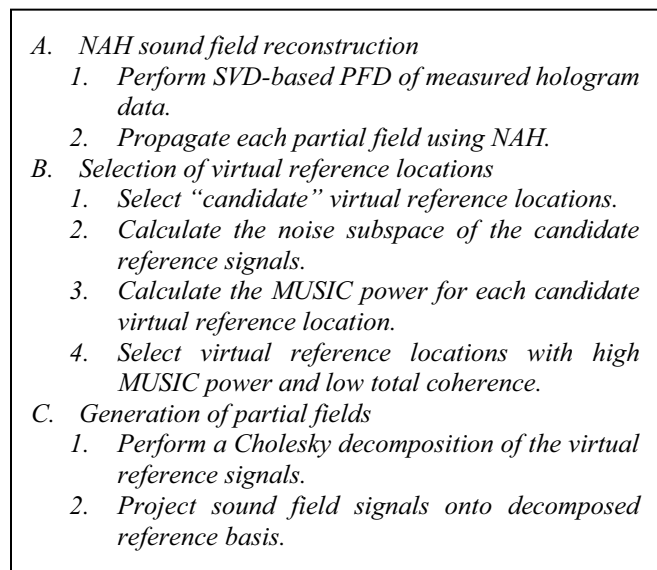
- 
- A. *NAH sound field reconstruction*
 - 1. *Perform SVD-based PFD of measured hologram data.*
 - 2. *Propagate each partial field using NAH.*
 - B. *Selection of virtual reference locations*
 - 1. *Select "candidate" virtual reference locations.*
 - 2. *Calculate the noise subspace of the candidate reference signals.*
 - 3. *Calculate the MUSIC power for each candidate virtual reference location.*
 - 4. *Select virtual reference locations with high MUSIC power and low total coherence.*
 - C. *Generation of partial fields*
 - 1. *Perform a Cholesky decomposition of the virtual reference signals.*
 - 2. *Project sound field signals onto decomposed reference basis.*

Figure 1 Outline of the virtual reference methodology for generating physically meaningful partial fields.

2.1 NAH sound field reconstruction

The placement of virtual references in a given sound field requires the prediction of sound pressures at those virtual locations based on data measured elsewhere. Hence, the first step in the OLVR process is to perform an NAH reconstruction of the three-dimensional sound field in the proximity of the source. For sound fields generated by multiple, independent sources, a multi-reference PFD procedure must be used to obtain mutually incoherent partial fields before NAH is implemented. Although detailed descriptions of these methods are not provided here, the reader is directed to References 8 and 13 for the theoretical development of SVD-based PFD, and to References 3 and 18 for NAH.

In summary, SVD-based PFD provides mutually incoherent partial fields from a measured hologram. An SVD of the cross spectrum of measured reference signals is performed, resulting in a linearly independent basis. The singular vectors represent new reference signals, and the measured field is projected onto these new references, which generates a linearly independent set of partial fields, \mathbf{P} . The relative strengths of these partial

fields are ordered and monotonically decreasing. The virtual coherence method¹² is then used to obtain an estimate of the number of source-related partial fields, K , which is an important number in the noise estimation procedure of the following subsection.

Each partial field is propagated to a new location using NAH. The acoustic field on a reconstruction surface can be represented by

$$\mathbf{Y} = \mathbf{H}_{yp} \mathbf{P} , \quad (1)$$

where \mathbf{Y} is the matrix containing the entire set of partial fields reconstructed on the surface at all reconstruction locations, and \mathbf{H}_{yp} is the transfer matrix that relates field signals on the hologram and reconstruction surfaces. This transfer matrix represents the entire NAH back-propagation procedure,³ including spatial windowing and aperture extension,¹⁹ regularization,²⁰ etc. The reconstruction is repeated over multiple surfaces, each of which consists of a set of partial fields.

2.2 Selection of virtual references

The virtual reference signals are selected by the experimenter from the partial field signal matrices, evaluated at the reconstruction locations. Hence, virtual references can be placed anywhere in the sound field reconstructed by the NAH projection. If the location of each subsource is known, this is straightforward. The method of Kim *et al.*¹⁰ is an automated optimization method for selecting the locations of the virtual references, which is particularly useful if the exact source locations are unknown. It was successful in identifying the locations of numerical point sources and physical loudspeakers in an experiment, and in isolating the fields radiated by each of these sources. A variation of this method is implemented here to determine the optimal locations of virtual references in the jet-noise field.

From all possible reconstruction locations accessible through an NAH prediction of sound pressures in the field a subset of “candidate” virtual reference locations must be selected. Let the matrix \mathbf{Y} be limited to a representation of N such points. The intuitive approach is to select all points within a plausible source region. The implementation given in this paper limits the candidate locations to a single reconstruction plane near the source, but a volumetric region of candidate locations may be desirable in future investigations.¹⁰

The noise subspace must be estimated at all N locations, in preparation for the MUSIC power calculation. To do this, the cross-spectral matrix of the candidate reference signals,

$$\mathbf{S}_{yy} = \mathbf{Y}\mathbf{Y}^H , \quad (2)$$

is decomposed using an SVD to obtain

$$\mathbf{S}_{yy} = \mathbf{W}\mathbf{\Sigma}\mathbf{W}^H . \quad (3)$$

The unitary matrix, \mathbf{W} , can be expressed in terms of eigenvectors, i.e., $\mathbf{W} = [\mathbf{w}_1 \ \mathbf{w}_2 \ \cdots \ \mathbf{w}_N]$, where \mathbf{w}_n is the n th singular vector associated with the n th singular value. If there are K independent sources that generate the field, then there are K source-related eigenvectors and the noise subspace can be defined in terms of the noise-related eigenvectors, \mathbf{w}_n , ($n = K + 1$ to N), as

$$\mathbf{R}_{\text{noise}} = \sum_{n=K+1}^N \mathbf{w}_n \mathbf{w}_n^H . \quad (4)$$

With the noise subspace estimated, the MUSIC power can be calculated. All of the eigenvectors are orthogonal, so the signal subspace spanned by the source-related eigenvectors, \mathbf{w}_n ($n = 1$ to K), is orthogonal to the noise subspace. The calculation of the MUSIC power relies on this fact, which is the next step in the OLVR process. To obtain the MUSIC powers, it is first assumed that a source is located at the n th point on a reconstruction surface, which is represented by a “trial vector,”

$$\mathbf{u}_n = [0 \cdots 0 \ 1 \ 0 \cdots 0]^T . \quad (5)$$

The n th element of \mathbf{u}_n is unity, and all other $N-1$ elements are zero. The MUSIC power is then calculated in terms of the trial vectors and the noise subspace as

$$P_{\text{MUSIC}} = \frac{1}{\mathbf{u}^H \mathbf{R}_{\text{noise}} \mathbf{u}} . \quad (6)$$

Theoretically, the MUSIC power is infinite when $\mathbf{u} = \mathbf{w}_n$, $n = 1$ to K . In the case of trial vectors that approximate the eigenvectors, the MUSIC power is higher for trial vectors that most closely reflect actual source locations. The calculation of the MUSIC power is therefore repeated for all N candidate reference locations. The optimal virtual reference locations are those at which the MUSIC power is the highest.

Differences between the application of the MUSIC power calculation for traditional, localized sources¹⁰ and for jet-noise sources should be considered. The trial vector of Eq. 5 represents a point source located at the n th position. The application of such trial vectors for a sound field generated by discrete localized sources results in a map of MUSIC powers with discrete localized maxima. However, distributed, partially spatially coherent sources, such as jets, result in spatially extended regions of high MUSIC powers. Sound pressure signals in these regions can be highly coherent, resulting in redundant virtual reference signals. Therefore, a way is provided to remove redundant virtual reference locations, described below. Alternative trial vectors that represent distributed sources could be developed—a study which merits further investigation.

The removal of redundant virtual reference signals begins by placing virtual references at *all* candidate reconstruction locations. Then, from the candidate-virtual-reference cross-spectral matrix, $\mathbf{S}_{\mathbf{x}'\mathbf{x}'} = \mathbf{X}'\mathbf{X}'^H$, the coherence between signals i and j can be calculated as

$$\gamma_{ij}^2 = \frac{|S_{ij}|^2}{S_{ii}S_{jj}} , \quad (7)$$

where S_{ii} and S_{jj} are the autospectra of references i and j , respectively, and S_{ij} is the cross spectrum between the two. If the coherence between two candidate source locations is nearly unity, then the sources are coherent and the reference at the location of smaller MUSIC power should be removed. This is repeated until the remaining virtual references are incoherent and equal in number to the number of incoherent subsources. For sound fields of high coherence over large spatial regions, which gradually tapers away from a maximum, a coherence

threshold is selected, and all but the one virtual reference with the maximum MUSIC power from within the region of high coherence is discarded. The coherence threshold can be selected such that exactly K virtual reference locations remain after the redundancy removal process. The result is a set of K reference signals, sorted in order of highest to lowest MUSIC powers, and low mutual coherence.

The next step is to obtain the virtual reference signal matrix. It is calculated

$$\mathbf{X} = \begin{bmatrix} \mathbf{c}_1^T \mathbf{Y}_1 \\ \mathbf{c}_2^T \mathbf{Y}_2 \\ \vdots \\ \mathbf{c}_k^T \mathbf{Y}_k \end{bmatrix} \quad (8)$$

where \mathbf{X} is the K by K virtual reference signal matrix. Paraphrasing Kim *et al.*,¹⁰ in Eq. 8, \mathbf{c}_m “represents the N by 1 reference selection vector: when the m th virtual reference is positioned at the i th field position on the reconstruction surface, all elements of \mathbf{c}_m are zeros, except for the element at the i th row, which is itself unity. Note that the matrix $\mathbf{Y}_m \dots$ represents the partial field signal matrix on the reconstruction surface at which the m th virtual reference is placed, and that the vector, \mathbf{c}_m , denotes the m th virtual reference location on the m th reconstruction surface. Thus, the location of the m th reconstruction surface in combination with the vector, \mathbf{c}_m , determines the location of the m th virtual reference in a three-dimensional space.” In essence, \mathbf{X} is comprised of the selected signals from \mathbf{Y} , corresponding to the virtual reference locations.

2.3 Generation of partial fields

With virtual references selected, they can then be decomposed to form a linearly independent basis set. This is performed with the PCD method. A rigorous mathematical derivation of the PCD technique is provided by Bendat.¹⁷ Hallman and Bolton²¹ provide a comparison of SVD-based PFD (sometimes called the “virtual coherence” method) and PCD. Here, a Cholesky decomposition of the virtual reference signals is used to perform the PCD, represented by

$$\mathbf{S}_{xx} = \mathbf{X}\mathbf{X}^H = \mathbf{L}\mathbf{L}^H, \quad (9)$$

where \mathbf{L} is a lower triangular matrix containing the now linearly independent basis signal vectors. In essence, all information in the virtual reference set that is coherent with the first reference signal is taken as the first basis signal. This is then subtracted from the remaining virtual reference signals. A second reference signal is then chosen, and all remaining information that is coherent with this signal is removed from the set, and so on. Hence, Cholesky decomposition represents an iterative allocation and removal of virtual reference signal energy.

Finally, the partial fields are generated from the basis set of the virtual reference signals. The cross spectral matrix between all field signals and virtual reference signals is calculated,

$$\mathbf{S}_{xy} = \mathbf{X}\mathbf{Y}^H. \quad (10)$$

The partial fields are obtained with

$$\mathbf{P}_x = \mathbf{S}_{xy}^H \mathbf{L}^{H^{-1}} . \quad (11)$$

These partial fields represent the physical partial fields radiated by independent subsource insomuch as each virtual reference senses one and only one independent subsource.

3. Experiment

To demonstrate its utility, OLVR was applied to NAH measurements of a full-scale jet. Sound pressures in the near field of a jet on a Lockheed Martin/Boeing F-22A Raptor were recorded with a 5 x 18 array of microphones, which had 0.15 cm (6 in.) spacing. An approximately 2 x 24 m vertical planar region 5.6 m from the shear layer was scanned, which measurement was used as the hologram for NAH (see plane 2 in Fig. 2). In addition, 50 fixed reference microphones (blue dots in Fig. 2) were placed on the ground with 0.6 m (2 ft.) spacing, spanning more than 30 m. Measurements were repeated for four engine conditions ranging from idle to full afterburner. The results of this paper focus on military engine powers.

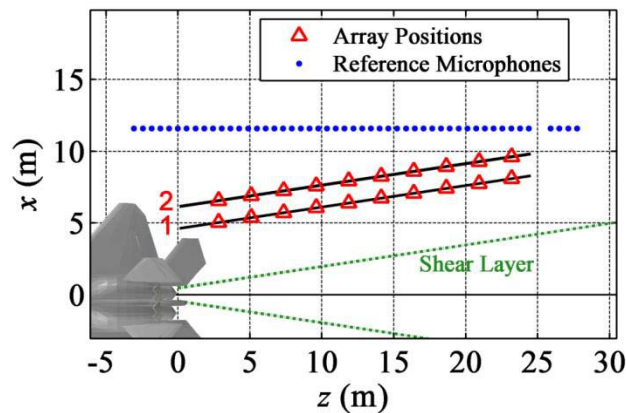


Figure 2 Schematic of the hologram measurements relative to the aircraft. Locations of the field array are marked by red triangles. Blue dots show the location of the reference array. Plane 2, which is the measurement used for NAH in this work, has a perpendicular distance of 5.6 m from the approximate shear layer location.

4. Results and Discussion

A discussion of the SVD-based PFD method and the NAH processing used in this work may be found in References 9 and 3, respectively. Selected results are shown here. For example, the partial fields from SVD-based PFD are shown in Fig. 3 for 105 Hz, and in Fig. 4 for 210 Hz. (The maximum frequency of the spectrum in the downstream direction is near 105 Hz, and 210 Hz was selected because it is double that.) Parts (a) of each figure show the total measured SPLs at plane 2. Parts (b) show the first four partial fields (out of 50, total). Note how energy is “packed” into the first partial fields in each case, due to the SVD. This demonstrates how SVD-based PFD provides a method for estimating the number of independent source mechanisms, K , based on the number of partial fields with significant energy. A comparison of these two figures demonstrates the trend that jet noise at higher frequencies is comprised of more independent sources. From a criterion that each

“significant” partial field must contain levels within 30 dB of the maximum measured level, it was determined for these data that $K = 2$ in the 105 Hz case and $K = 6$ in the 210 Hz case.

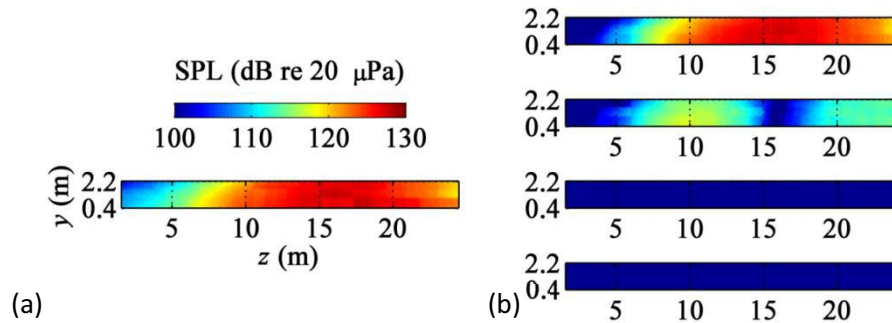


Figure 3 (a) Total measured SPLs at plane 2 for 105 Hz. (b) First four partial fields from SVD-based PFD.

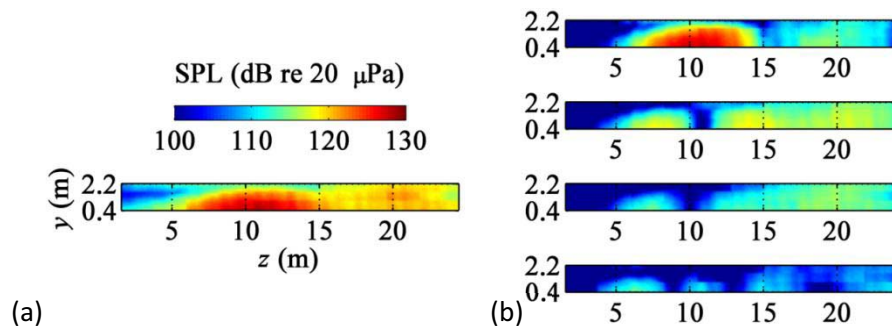


Figure 4 Left: Total measured SPLs at plane 2 for 210 Hz. Right: First four partial fields from SVD-based PFD.

NAH was implemented on these mutually incoherent partial fields. The reconstructed sound pressure levels (SPLs) at the approximate shear layer location are shown in Fig. 5. The black lines on each plot mark the locations where the levels are 3 decibels below the maximum level for each frequency. Such an analysis provides insight about source characteristics as a function of frequency, engine condition, etc. NAH reconstructions can be repeated for multiple locations, providing three-dimensional sound field visualization, such as those shown in Figs. 6 and 7. The reconstruction of the field at 105 Hz demonstrates a large main lobe radiating in a preferred aft direction. The main lobe at 210 Hz radiates slightly more in the forward direction, and is narrower. In addition, a secondary lobe has emerged in the far aft direction. This secondary lobe does not appear in laboratory-scale jet-noise measurements, and the source of this lobe is unclear. The coherence of these two lobes is investigated here to demonstrate the utility of OLVR, and hence, many of the following results are for the 210 Hz data.

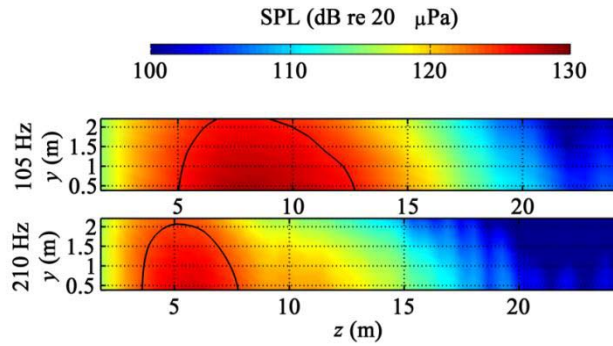


Figure 5 Reconstructed SPLs at the shear layer, after the application of NAH to the measured data, for 105 and 210 Hz. Black lines mark the regions containing levels within three decibels of the maximum level for each respective frequency.

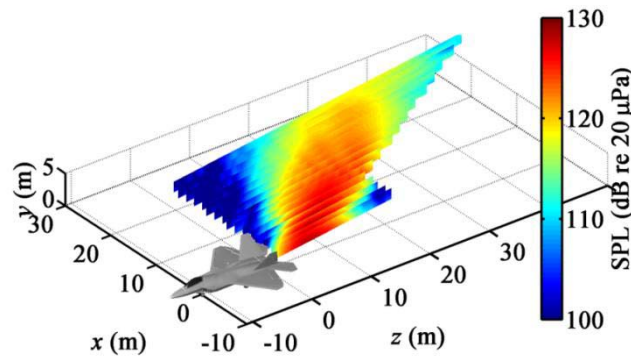


Figure 6 Three-dimensional NAH sound field reconstruction for 105 Hz.

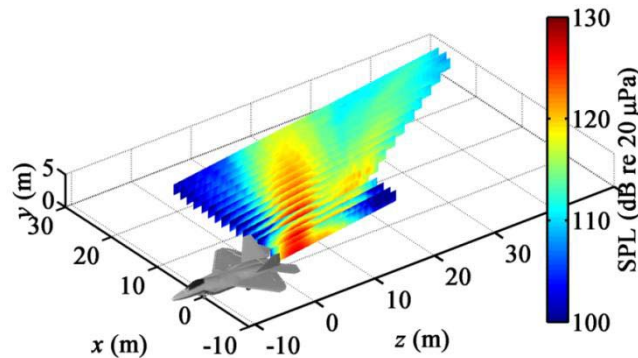


Figure 7 Three-dimensional NAH sound field reconstruction for 210 Hz.

For the selection of candidate virtual reference locations it is desirable to choose locations in a three-dimensional volumetric region, allowing for volumetric distribution of sources.¹⁰ In this initial application of OLVR to the full-scale jet data the candidate locations are restricted to the shear-layer reconstruction plane, the data for which are shown in Fig. 5. The calculated MUSIC powers at these respective locations for the 210 Hz case are shown in

Fig. 8. Note the broad regions of high MUSIC power, demonstrating the spatial coherence of the source and the need for a redundancy-removal process.

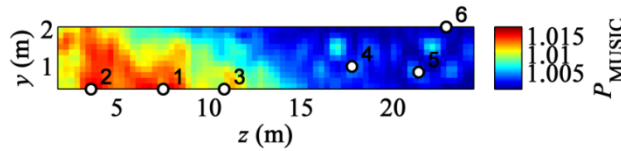


Figure 8 MUSIC powers calculated over the shear-layer reconstruction surface for 210 Hz. Markers show the locations of the $K = 6$ virtual references after the redundancy-removal process.

The markers on Fig. 8 show the end-result locations of the six virtual references, after redundancy removal was implemented. Here, a coherence threshold of 0.4 resulted in the necessary $K = 6$ virtual references. They are appropriately spread out and located near localized maxima of MUSIC powers. Figure 9 shows how the coherence between all the resulting virtual references is below the 0.4 threshold.

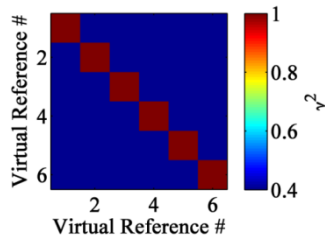


Figure 9 Ordinary coherence between the six virtual reference signals for the 210 Hz case. A coherence threshold of 0.4 was selected for the redundancy-removal process in the 210 Hz case.

The Cholesky decomposition of the virtual reference signals is demonstrated in Fig. 10. The level magnitudes of the virtual reference signals, \mathbf{X} , are shown in Fig. 10a. The decomposed signals, \mathbf{L} , are shown in Fig. 10b. Their linear independence is clearly demonstrated. In addition, it is shown that most of the signal energy is contained in the first three signals. There is a significant drop in energy between the third and fourth signals, such that the last three signals are not visible on the color scale of this figure.

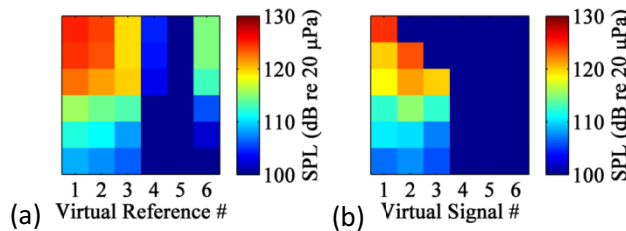


Figure 10 (a) Six virtual reference signals, \mathbf{X} , (magnitude in decibels) for the 210 Hz case. (b) Cholesky-decomposed virtual reference signals, \mathbf{L} .

Figure 11 shows the two partial fields (PFs) that are generated with OLVR for the 105 Hz jet data. The white dots mark the locations of the virtual references, so the PFs that result from them are somewhat intuitive. This decomposition confirms that, at this low frequency, the main lobe is radiated by one dominant source. Some low-magnitude

information is contained in a second PF, demonstrating that the main source is not perfectly coherent. The seemingly missing energy in the second partial field is due to a non-optimized NAH propagation,³ which will be corrected in future studies.

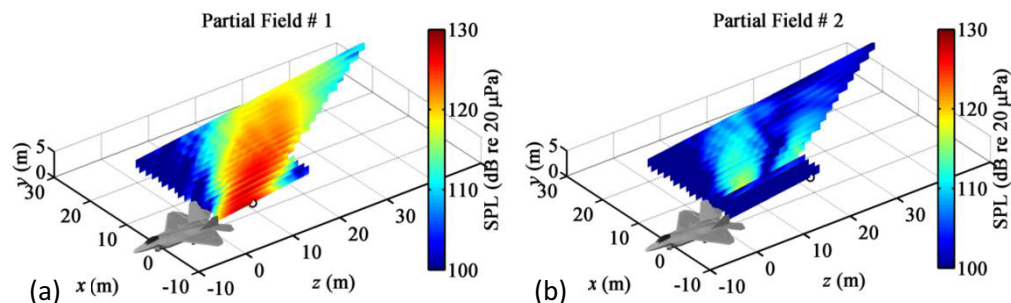


Figure 11 The (a) first, and (b) second partial fields generated from OLVR on jet noise data at 105 Hz. Markers show the location of each respective virtual reference.

The OLVR decomposition of the jet at military conditions and 210 Hz is shown in Fig. 12. The first four PFs, out of six, are shown. Note first how the main lobe at 210 Hz has been split into two nearly equal-magnitude components between PF-1 and PF-2. This demonstrates that the source generating this lobe is not entirely coherent. It might even be considered two “coherence lengths” wide, although a quantitative definition of a coherence length merits further investigation.^{22,23} The second thing to note is how, as the main lobe nearly vanishes by PF-1, the secondary lobe gradually increases in magnitude from PF-1 to PF-2, and again to PF-3. Some of the energy from the secondary lobe is contained in the first two PFs. This may be due, in part, to “leakage”, or the fact that even a well-placed virtual reference senses some information from multiple source mechanisms. Thus, although there may be some partial coherence between the sources generating these two lobes, overall they are independent. In addition, there is a significant drop in energy between the third and fourth partial fields, consistent with the decomposed reference vectors of Fig. 10b.

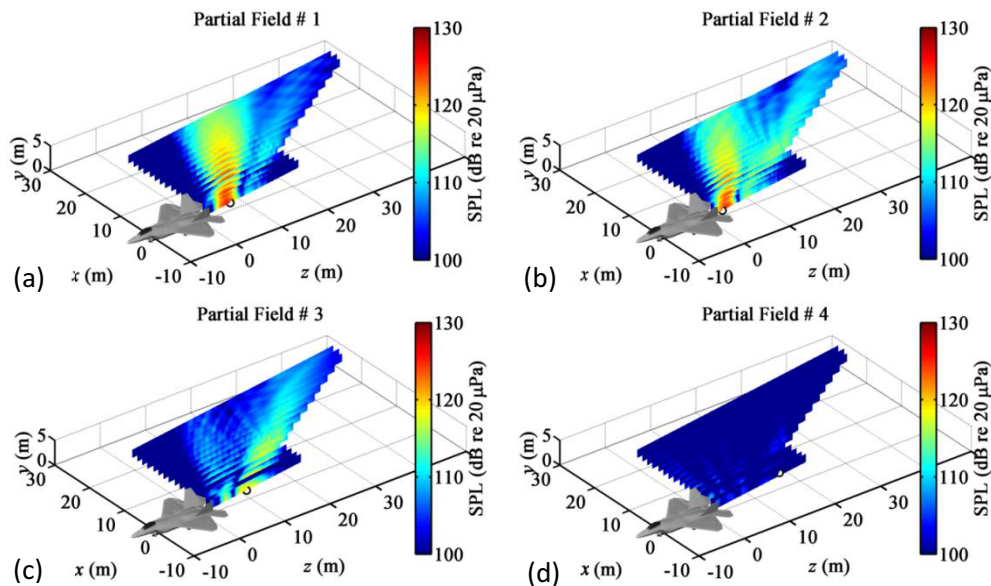


Figure 12 The (a) first, (b) second, (c) third, and (d) fourth partial fields generated from OLVR on jet noise data at 210 Hz. Markers show the location of each respective virtual reference.

5. Conclusion

The optimized-location virtual reference method (OLVR) for partial field decomposition of jet noise sources has been explained in this paper. OLVR is shown to generate a set of partial fields for a full-scale jet noise source that were intuitive and physically meaningful. The resulting partial fields from this method demonstrate the partial spatial coherence of the source. It provides not only an estimate of the number of independent sources, but also an indication of their various locations and the source spatial coherence lengths. For the sources at 210 Hz, with the engine operating at military conditions, it was shown that the two radiation lobes were generated by independent source mechanisms. In the future, detailed application of OLVR to the jet noise field can provide extensive information about source distributions and coherence properties as a function of frequency and engine operation conditions.

Acknowledgments

The authors would like to thank Richard McKinley and Robert McKinley with the Air Force Research Laboratory, as well as the Office of Naval Research for their support. This research was supported in part by the appointment of Alan Wall to the Student Research Participation Program at U.S. Air Force Research Laboratory, Human Effectiveness Directorate, Warfighter Interface Division, Battlespace Acoustics administered by the Oak Ridge Institute for Science and Education through an interagency agreement between the U.S. Department of Energy and USAFRL.

SBIR DATA RIGHTS - (DFARS 252.227-7018 (JUNE 1995)); Contract Number: [FA8650-08-C-6843](#); Contractor Name & Address: [Blue Ridge Research and Consulting, LLC, 15 W Walnut St., Suite C; Asheville, NC](#); Expiration of SBIR Data Rights Period: [March 17, 2016](#) (Subject to SBA SBIR Directive of September 24, 2002); Clearance

Date: April 16, 2012. *The Government's rights to use, modify, reproduce, release, perform, display, or disclose technical data or computer software marked with this legend are restricted during the period shown as provided in paragraph (b)(4) of the Rights in Noncommercial Technical Data and Computer Software—Small Business Innovation Research (SBIR) Program clause contained in the above identified contract. No restrictions apply after the expiration date shown above. Any reproduction of technical data, computer software, or portions thereof marked with this legend must also reproduce the markings.*

References

- ¹D. Otte, P. Sas and P. V. Ponsele, "Noise source identification by use of principal component analysis," Proceedings of Inter-Noise 88, pp. 199, 1988.
- ²D. Otte, P. Sas, R. Snoeys, P. V. Ponsele and J. Leuridan, "Use of principal component analysis and virtual coherences for dominant noise source identification," Proceedings of Second International Seminar on Noise Source Identification and Numerical Methods in Acoustics, 1987.
- ³A. T. Wall, K. L. Gee, T. B. Neilsen, D. W. Krueger, M. M. James, S. D. Sommerfeldt and J. D. Blotter, "Full-scale jet noise characterization using scan-based acoustical holography," AIAA Paper 2012-2081, June 4-6, 2012.
- ⁴P. N. Shah, H. Vold and M. Yang, "Reconstruction of far-field noise using multireference acoustical holography measurements of high-speed jets," AIAA Paper 2011-2772, June 5-8, 2011.
- ⁵H. Vold, P. N. Shah, J. Davis, P. G. Bremner, D. McLaughlin, P. Morris, J. Veltin and R. McKinley, "High-resolution continuous scan acoustical holography applied to high-speed jet noise," AIAA Paper 2010-3754, June 7-9, 2010.
- ⁶M. Lee and J. S. Bolton, "Source characterization of a subsonic jet by using near-field acoustical holography," J. Acoust. Soc. Am. **121**, 967-977 (2007).
- ⁷D. Long, J. Peters and M. Anderson, "Evaluating turbofan exhaust noise and source characteristics from near field measurements," AIAA Paper 2009-3214, May 11-13, 2009.
- ⁸M. Lee and J. S. Bolton, "Scan-based near-field acoustical holography and partial field decomposition in the presence of noise and source level variation," J. Acoust. Soc. Am. **119**, 382-393 (2006).
- ⁹A. T. Wall, K. L. Gee, M. D. Gardner, T. B. Neilsen and M. M. James, "Near-field acoustical holography applied to high-performance jet aircraft noise," Proc. Mtgs. Acoust. **9**, 040009 (2011).
- ¹⁰Y. J. Kim, J. S. Bolton and H. S. Kwon, "Partial sound field decomposition in multireference near-field acoustical holography by using optimally located virtual references," J. Acoust. Soc. Am. **115**, 1641-1652 (2004).
- ¹¹K.-U. Nam and Y.-H. Kim, "Visualization of multiple incoherent sources by the backward prediction of near-field acoustic holography," J. Acoust. Soc. Am. **109**, 1808-1816 (2001).
- ¹²S. M. Price and R. J. Bernhard, "Virtual coherence: A digital signal processing technique for incoherent source identification," Proceedings of 4th International Modal Analysis Conference, pp. 1256-1262, 1986.
- ¹³J. Hald, "STSF—A unique technique for scan-based nearfield acoustical holography without restriction on coherence," Technical Report No. 1, from Bruel & Kjaer, Naerum, Denmark, 1989.
- ¹⁴D. H. Johnson and D. E. Dudgeon, *Array signal processing: Concepts and techniques* (Prentice-Hall, 1993).
- ¹⁵A. T. Wall, K. L. Gee, M. M. James, K. A. Bradley, S. A. McNerny and T. B. Neilsen, "Near-field noise measurements of a high-performance military jet aircraft," Noise Control Eng. J. **60**, 421-434 (2012).
- ¹⁶M. M. James and K. L. Gee, "Aircraft jet plume source noise measurement system," Sound Vib. **44**, 14-17 (2010).
- ¹⁷J. S. Bendat, "Modern analysis procedures for multiple input/output problems," J. Acoust. Soc. Am. **68**, 498-503 (1980).
- ¹⁸J. Hald, "Basic theory and properties of statistically optimized near-field acoustical holography," J. Acoust. Soc. Am. **125**, 2105-2120 (2009).
- ¹⁹A. T. Wall, K. L. Gee, D. W. Krueger, T. B. Neilsen and M. M. James, "Aperture extension for near-field acoustical holography applied to jet noise," J. Acoust. Soc. Am. **130**, 2344 (2011).
- ²⁰E. G. Williams, "Regularization methods for near-field acoustical holography," J. Acoust. Soc. Am. **110**, 1976-1988 (2001).
- ²¹H. S. Kwon and J. S. Bolton, "Partial field decomposition in nearfield acoustical holography by the use of singular value decomposition and partial coherence procedures," Proceedings of NOISE-CON, pp. 649-654, 1998.
- ²²A. T. Wall, K. L. Gee and T. B. Neilsen, "On near-field acoustical inverse measurements of partially coherent sources," Proc. Mtgs. Acoust. **11**, 040007 (2012).
- ²³A. T. Wall, M. D. Gardner, K. L. Gee and T. B. Neilsen, "Coherence length as a figure of merit in multireference near-field acoustical holography," J. Acoust. Soc. Am. **132**, EL215-EL221 (2012).